

Conditions under which a supercritical turbidity current traverses an abrupt transition to vanishing bed slope without a hydraulic jump

By SVETLANA KOSTIC AND GARY PARKER

St. Anthony Falls Laboratory, University of Minnesota, Minneapolis MN 55414 USA

kost0067@umn.edu; parke002@umn.edu

Turbidity currents act to sculpt the submarine environment through sediment erosion and deposition. A sufficiently swift turbidity current on a steep slope can be expected to be supercritical in the sense of the bulk Richardson number; a sufficiently tranquil turbidity current on a mild slope can be expected to be subcritical. The transition from supercritical to subcritical flow is accomplished through an internal hydraulic jump. Consider a turbidity current flowing from a steep canyon onto a milder fan, and then exiting the fan down another steep canyon. The flow might be expected to a) undergo a hydraulic jump to subcritical flow near the canyon-fan break, and then b) accelerate again to critical flow at the fan-canyon break downstream. The problem of locating the hydraulic jump is here termed the “jump problem.” Experiments with fine-grained sediment have confirmed the expected behavior outlined above. Similar experiments with coarse-grained sediment suggest that if the deposition rate is sufficiently high, this “jump problem” may have no solution with the expected behavior, and in particular no solution with a hydraulic jump. In such cases the flow either transits the length of the low-slope fan as a supercritical flow and shoots off the fan-canyon break without responding to it, or dissipates as a supercritical flow before exiting the fan. The analysis presented below confirms the existence of a range associated with rapid sediment deposition where no solution to the “jump problem” can be found. The criterion for this range is stated in terms of an order-one dimensionless parameter involving the fall velocity of the sediment. The criterion is tested and confirmed against the experiments mentioned above. A sample field application is presented.

1. Introduction

The fluid dynamics of turbidity currents, which are dense bottom underflows driven by suspended sediment, has attracted considerable interest in recent years (e.g. Hallworth et al., 1998; Bonnecaze & Lister, 1999; Maxworthy, 1999; Gladstone & Woods, 2000). Turbidity currents are close relatives of underflows driven by e.g. thermohaline effects, such as the underflow of dense, salty water across the Gibraltar Sill from the Mediterranean Sea into the Atlantic (e.g. Armi & Farmer, 1988; Lane-Serff et al., 2000). Turbidity currents differ from such thermohaline flows in that the agent of the excess density, i.e. sediment, is not a conserved quantity. Sediment is free to deposit on the bed or be entrained from it in accordance with the dictates of the flow-sediment interaction. As a result, turbidity currents behave differently from conservative dense bottom underflows in several key ways. This paper is devoted to one of those differences.

Turbidity currents are responsible for the creation of rather spectacular deep-sea morphologies. On steeper slopes they can carve submarine canyons that are 100's of

meters deep; on shallower slopes they can deposit submarine fans over 10's or 100's of km. The image of Figure 1 shows an example of such a morphology. The continental slope off the delta of the Niger River, Africa shows a dip (down-slope) profile with repeated undulations in bed slope. Turbidity currents have excavated canyons into the steeper zones and deposited small submarine fans in the shallower zones. In Figure 1, an upstream canyon debouches onto a fan of much lower slope; the fan ends in another canyon where slope again increases.

A key parameter governing the dynamics of dense bottom flows is the bulk Richardson number \mathbf{Ri} (e.g. Ellison & Turner, 1959), where $\mathbf{Ri} = RgCh/U^2$ and U denotes layer-averaged flow velocity, C denotes layer-averaged volume concentration of suspended sediment, h denotes layer thickness, g denotes the acceleration of gravity and R denotes the submerged specific gravity of sediment, equal to 1.65 for quartz. (More formal definitions follow below.) Flows for which $\mathbf{Ri} < 1$ are swift, supercritical flows; flows for which $\mathbf{Ri} > 1$ are tranquil, subcritical flows. It is reasonable to expect that the turbidity currents that formed the morphology of Figure 1 might have been supercritical in the canyons and subcritical on the fan.

In order to make the transition from supercritical to subcritical flow, a dense bottom flow must generally undergo an internal hydraulic jump (e.g. Yih and Guha, 1955). Many sedimentologists have tried to infer such jumps from the sedimentary patterns visible in outcrops (e.g. Mutti, 1977; Russell & Arnott, 2003). The only direct knowledge of internal hydraulic jumps due to turbidity currents, however, comes from experiments.

Perhaps the first comprehensive set of experiments on turbidity currents undergoing hydraulic jumps were those of Garcia (1989, 1993) and Garcia & Parker (1989). The configuration of the experiments is shown in Figure 2. The currents were quasi-steady. They flowed from a submerged sluice gate onto a region with a bed slope S of 0.08. At a distance of 5 m from the inlet point the bed slope dropped to zero; this region extended for another 6.6 m to a submerged free overfall, where the turbidity current debouched into a damping tank.

The geometry of Figure 2 can be thought of as a 1D analog of the 2D configuration of Figure 1. The sloping region in Figure 2 is analogous to the upstream canyon of Figure 1; the horizontal region in Figure 2 is analogous to the fan in Figure 1, and the free overfall at the downstream end of Figure 2 is analogous to the canyon at the downstream end of the fan in Figure 1.

Garcia (1989, 1993) used four grades of sediment in order to study the dynamics of net-depositional turbidity currents at slope breaks. In the case of the two finer grades of sediment, 4 μm material (NOVA) and 9 μm material (DAPER), supercritical flows emanating from the inlet underwent a hydraulic jump near the slope break. The subcritical flow downstream then accelerated in the vicinity of the free overfall and debouched into it. A subcritical dense underflow passing a free overfall must attain a critical Richardson number; for most purposes this critical value can be approximated as

unity. The general pattern of flow observed in the NOVA and DAPER runs is schematized by the solid line of Figure 2.

In the case of otherwise similar experiments with coarser sediment, i.e. 30 μm material (GLASSA), the hydraulic jump was barely if at all manifested. In the case of 65 μm sediment (GLASSB), a hydraulic jump was clearly absent. The absence of the hydraulic jump has been confirmed by the numerical simulations of Choi & Garcia (1995) and Kostic & Parker (2004; submitted).

One possibility is that the length of the horizontal domain of the experiments of Garcia (1989, 1993) was simply too short for a hydraulic jump in the case of the coarser sediments. A second possibility, however, is that no jump is possible when the sediment is “sufficiently coarse” in some dimensionless sense.

This speculation allows articulation of the “jump problem.” Consider a supercritical turbidity current debouching onto a domain of horizontal bed ending in a free overfall. Is there any length L of the horizontal domain that allows a hydraulic jump to subcritical flow within it, such that this subcritical flow attains the critical condition in Richardson number at $x = L$?

It is shown below that for the case of a conservative dense underflow the “jump problem” always has a solution. It is possible to specify a value of L that is too short for a hydraulic jump, in which case the supercritical flow shoots off the free overfall without responding to it, as shown in Figure 2. If L is allowed to be a free variable, however, a range of values of L for which a hydraulic jump will occur on the domain can always be found.

The essential result of the analysis presented below is the conclusion that in the case of turbidity currents undergoing sufficiently rapid deposition the “jump problem” has no solution, regardless of the length L . In such cases the turbidity current will either flow off the end of the domain for sufficiently short values of L , or dissipate as a supercritical flow within the domain for sufficiently long values of L . A simple dimensionless criterion discriminating between regions where the “jump problem” has a solution and where it does not is derived.

2. Governing equations

A turbidity current is a dense bottom underflow driven by the presence of suspended sediment in the water column. The suspended sediment renders the bottom underflow denser than the ambient water above, and thus drives the current down the bottom slope. Here the case of a turbidity current driven by a dilute suspension of sediment is considered. For simplicity it is assumed that the flow is driven only by sediment, so that there is no difference between the temperature or salinity of the water in the underflow and the ambient water above. The ambient water is assumed to be in hydrostatic equilibrium.

The equations governing a turbidity current can be expressed at a variety of levels of complexity, ranging from the box model of e.g. Gladstone & Woods (2000) to the full turbulence closure scheme of e.g. Felix (2001). Here the layer-averaged approach of Parker et al. (1986) is employed. Let x denote a boundary-attached streamwise coordinate and y denote a coordinate orthogonal to x and thus directed upward normal from the bed. The streamwise flow velocity averaged over turbulence is denoted as u , and the volume concentration of suspended sediment averaged over turbulence is denoted as c . Since the ambient water is in hydrostatic equilibrium, it can be assumed that $u \rightarrow 0$ and $c \rightarrow 0$ as $y \rightarrow \infty$. The flow is taken to be uniform in the transverse direction.

Layer-averaged flow velocity and concentration are denoted as U and C , respectively, where

$$U^2 h = \int_0^\infty u^2 dy \quad (2.1a)$$

$$U h = \int_0^\infty u dy \quad (2.1b)$$

$$U C h = \int_0^\infty u c dy \quad (2.1c)$$

and h denotes layer thickness. Parker et al. (1986) (see also Baines, 1999) obtain the following forms for layer-integrated balance of momentum, flow mass and mass of suspended sediment;

$$\frac{\partial U h}{\partial t} + \frac{\partial U^2 h}{\partial x} = -\frac{1}{2} R g \frac{\partial C h^2}{\partial x} + R g C h S - u_*^2 \quad (2.2a)$$

$$\frac{\partial h}{\partial t} + \frac{\partial U h}{\partial x} = e_w U \quad (2.2b)$$

$$\frac{\partial C h}{\partial t} + \frac{\partial U C h}{\partial x} = v_s (e_s - c_b) \quad (2.2c)$$

In the above equations S denotes streamwise bed slope and the parameter R , or submerged specific gravity of sediment, is given as

$$R = \frac{\rho_s}{\rho} - 1 \quad (2.3)$$

where ρ_s denotes the density of sediment and ρ denotes the density of sediment-free water. In addition, v_s denotes the fall velocity of the suspended sediment, which is characterized in terms of a single size for simplicity. The parameters u_* , e_w and e_s denote bed shear velocity, dimensionless coefficient of entrainment of ambient water from above, and dimensionless coefficient entrainment of sediment from the bed respectively. Finally, c_b denotes a near-bed value of concentration C .

In point of fact (2.2a) – (2.2c) include several order-one shape factors. For example, the term $RgChS$ in (2.2a) is more accurately written as $\alpha RgChS$, where

$$\alpha = \int_0^{\infty} f_c d\xi \quad , \quad f_c = \frac{c}{C} \quad , \quad \xi = \frac{y}{h} \quad (2.4a,b,c)$$

All the shape factors take the value of unity for a top-hat assumption for velocity and concentration profiles, i.e.

$$\frac{u}{U} = \frac{c}{C} = \begin{cases} 1 & , \quad 0 \leq \xi \leq 1 \\ 0 & , \quad 1 < \xi \end{cases} \quad (2.5)$$

Parker et al. (1987) and Garcia (1989) have evaluated the relevant shape factors for a range of experimental turbidity currents and found values not far from unity. Here the shape factors are set to unity as a matter of simplicity.

Equations (2.2a) – (2.2c) are closed by means of assumptions for shear velocity u_* , coefficient of water entrainment e_w , near-bed suspended sediment concentration c_b and coefficient of sediment entrainment e_s . Shear velocity u_* is related to layer-averaged flow velocity U by means of a dimensionless bed friction coefficient c_f , so that

$$u_*^2 = c_f U^2 \quad (2.6)$$

Here c_f is approximated as a specified constant. Water entrainment is specified in terms of the empirical relation of Fukushima et al. (1985);

$$e_w = \frac{0.00153}{0.0204 + \mathbf{Ri}} \quad (2.7)$$

where \mathbf{Ri} denotes a bulk Richardson number, defined as

$$\mathbf{Ri} = \frac{RgCh}{U^2} = \frac{Rgq}{U^3} \quad (2.8)$$

In the above equation q denotes the volume transport rate of suspended sediment per unit width, given by the relation

$$q = UCh \quad (2.9)$$

Near-bed sediment concentration c_b is related to the layer-averaged value C as

$$c_b = r_o C \quad (2.10)$$

where $r_o \geq 1$ is a dimensionless coefficient, with the equality holding only for the case of the top-hat assumption. In general r_o is a function of the flow (Parker, 1982). Here it is approximated as a constant for simplicity, an assumption that can be generalized at a future time.

Now consider the case of steady current that is free to develop in the streamwise direction. For this case (2.2a) – (2.2c) reduce with the aid of (2.6), (2.9) and (2.10) to the following forms for gradually varied flow.

$$\frac{dU}{dx} = \frac{\mathbf{Ri}S - e_w \left(1 + \frac{1}{2} \mathbf{Ri}\right) - c_f + \frac{1}{2} \mathbf{Ri} r_o \left(1 - \frac{U e_s h}{r_o q}\right) \frac{v_s}{U}}{1 - \mathbf{Ri}} \frac{U}{h} \quad (2.11a)$$

$$\frac{dh}{dx} = \frac{-\mathbf{Ri}S + e_w \left(2 - \frac{1}{2} \mathbf{Ri}\right) + c_f - \frac{1}{2} \mathbf{Ri} r_o \left(1 - \frac{U e_s h}{r_o q}\right) \frac{v_s}{U}}{1 - \mathbf{Ri}} \quad (2.11b)$$

$$\frac{dq}{dx} = -r_o \frac{q}{h} \left(1 - \frac{U e_s h}{r_o q}\right) \frac{v_s}{U} \quad (2.11c)$$

The research reported here focuses on a purely depositional turbidity current, for which e_s vanishes. This assumption follows the tradition of a considerable body of literature on turbidity currents and related flows containing particulate material, including e.g. Hallworth et al. (1998), Maxworthy (1999), Gladstone and Woods (2000) and Kostic and Parker (2003a,b).

3. Purely depositional supercritical turbidity current flowing into a zone of vanishing bed slope

The goal of the analysis presented here is the delineation of conditions for which a turbidity current does not undergo a hydraulic jump near a slope break no matter how long is the length L of the horizontal region of Figure 2. Now consider the configuration of the same Figure 2. If a supercritical turbidity current is to pass the break in slope and onto the zone of vanishing slope without undergoing a hydraulic jump to subcritical flow, it follows that the turbidity current must still be supercritical by the time it reaches the break in slope. That is, taking origin for the streamwise coordinate to be the break in slope, it follows that

$$\mathbf{Ri}_o \equiv \mathbf{Ri}|_{x=0} < 1 \quad (3.1)$$

Bed slope S vanishes on the domain $x \geq 0$. If in addition the turbidity current is assumed to be purely depositional ($e_s = 0$), (2.11a) – (2.11c) reduce to the forms

$$\frac{dU}{dx} = \frac{-e_w \left(1 + \frac{1}{2} \mathbf{Ri}\right) - c_f + \frac{1}{2} \mathbf{Ri} r_o \frac{v_s}{U}}{1 - \mathbf{Ri}} \frac{U}{h} \quad (3.2a)$$

$$\frac{dh}{dx} = \frac{e_w \left(2 - \frac{1}{2} \mathbf{Ri}\right) + c_f - \frac{1}{2} \mathbf{Ri} r_o \frac{v_s}{U}}{1 - \mathbf{Ri}} \quad (3.2b)$$

$$\frac{dq}{dx} = -r_o \frac{v_s}{U} \frac{q}{h} \quad (3.2c)$$

The above equations are now made dimensionless using the velocity U_o , flow thickness h_o and sediment discharge q_o at $x = 0$ as follows. Hatted dimensionless versions of h , U , q and x are defined as

$$h = h_o \hat{h} \quad , \quad U = U_o \hat{U} \quad , \quad q = q_o \hat{q} \quad , \quad x = \frac{h_o}{c_f} \hat{x} \quad (3.3a,b,c,d)$$

Equations (3.2a) – (3.2c) thus transform into the respective forms

$$\frac{d\hat{U}}{d\hat{x}} = \frac{-1 - \frac{e_w}{c_f} \left(1 + \frac{1}{2} \mathbf{Ri}_o \frac{\hat{q}}{\hat{U}^3}\right) + \frac{1}{2} \mathbf{Ri}_o \frac{\hat{q}}{\hat{U}^4} \varphi}{1 - \mathbf{Ri}_o \frac{\hat{q}}{\hat{U}^3}} \frac{\hat{U}}{\hat{h}} \quad (3.4a)$$

$$\frac{d\hat{h}}{d\hat{x}} = \frac{1 + \frac{e_w}{c_f} \left(2 - \frac{1}{2} \mathbf{Ri}_o \frac{\hat{q}}{\hat{U}^3}\right) - \frac{1}{2} \mathbf{Ri}_o \frac{\hat{q}}{\hat{U}^4} \varphi}{1 - \mathbf{Ri}_o \frac{\hat{q}}{\hat{U}^3}} \quad (3.4b)$$

$$\frac{d\hat{q}}{d\hat{x}} = -\varphi \frac{\hat{q}}{\hat{U}\hat{h}} \quad (3.4c)$$

where

$$\mathbf{Ri} = \mathbf{Ri}_o \frac{\hat{q}}{\hat{U}^3} \quad , \quad \mathbf{Ri}_o = \frac{Rgq_o}{U_o^3} \quad (3.5a,b)$$

$$\varphi = r_o \frac{v_s}{c_f U_o} \quad (3.6)$$

The boundary conditions on (3.5a) – (3.5c) are

$$\hat{U} \Big|_{\hat{x}=0} = 1 \quad , \quad \hat{h} \Big|_{\hat{x}=0} = 1 \quad , \quad \hat{q} \Big|_{\hat{x}=0} = 1 \quad (3.7a,b,c)$$

As shown in Figure 2, the domain within which (3.4a) – (3.4c) are to be solved ends in a free overfall located at $x = L$. If the flow does indeed undergo a jump to a subcritical flow within the domain, then the bulk Richardson number must achieve the value of unity at the overfall. That is, the following condition must be satisfied if a hydraulic jump occurs within the domain;

$$\mathbf{Ri} \Big|_{\hat{x}=\hat{L}} = \mathbf{Ri}_o \left(\frac{\hat{q}}{\hat{U}^3} \right) \Big|_{\hat{x}=\hat{L}} = 1 \quad (3.8)$$

where

$$\hat{L} = c_f \frac{L}{h_o} \quad (3.9)$$

4. Case of a conservative density underflow

A conservative density underflow is one for which the agent of the density difference is conserved. This case is recovered from (3.4a) – (3.4c) by taking the limit $v_s \rightarrow 0$ (vanishing fall velocity of the sediment), resulting in the relations

$$\frac{d\hat{U}}{d\hat{x}} = \frac{-1 - \frac{e_w}{c_f} \left(1 + \frac{1}{2} \frac{\mathbf{Ri}_o}{\hat{U}^3} \right)}{1 - \frac{\mathbf{Ri}_o}{\hat{U}^3}} \frac{\hat{U}}{\hat{h}} \quad (4.1a)$$

$$\frac{d\hat{h}}{d\hat{x}} = \frac{1 + \frac{e_w}{c_f} \left(2 - \frac{1}{2} \frac{\mathbf{Ri}_o}{\hat{U}^3} \right)}{1 - \frac{\mathbf{Ri}_o}{\hat{U}^3}} \quad (4.1b)$$

where since $\hat{q} = 1$ everywhere

$$\mathbf{Ri} = \frac{\mathbf{Ri}_o}{\hat{U}^3} \quad (4.2)$$

An example of a conservative density underflow is one driven by excess density associated with thermohaline effects, in which case the following transformation is appropriate; where $\Delta\bar{\rho}$ denotes the layer-averaged excess density of the flow,

$$\mathbf{RC} \rightarrow \frac{\Delta\bar{\rho}}{\rho} \quad (4.3)$$

Although the case of a conservative density underflow has been studied extensively (e.g. Ellison and Turner, 1959), it is of use to review it before progressing to the non-conservative case.

The solution of (4.1a) and (4.1b) subject to (3.7a,b) on the domain of Figure 2 can be implemented as follows. Assuming that e_w is specified by (2.7), (4.1a) and (4.1b) can be solved subject to the initial conditions (3.7a) and (3.7b) for any specified value of upstream Richardson number \mathbf{Ri}_0 and friction coefficient c_f . Here the case $\mathbf{Ri}_0 < 1$ (supercritical flow upstream) is considered first. It is seen the numerator on the right-hand side of (4.1a) is always negative, whereas the denominator on the right-hand side of (4.1a) is positive. As a result \hat{U} must decrease monotonically in \hat{x} , in which case \mathbf{Ri} must increase in accordance with (4.2). When \hat{U} is reduced to the value

$$\hat{U} = (\mathbf{Ri}_0)^{1/3} \quad (4.4)$$

the Richardson number \mathbf{Ri} attains the value unity, and the denominators of both (4.1a) and (4.1b) become singular. The distance $\hat{L}_{\text{sup max}}$ at which this condition is reached defines the maximum possible length of a supercritical turbidity current emanating from the point $\hat{x} = 0$. Thus in general

$$\hat{L}_{\text{sup max}} = \hat{L}_{\text{sup max}}(\mathbf{Ri}_0, c_f) \quad (4.5)$$

This functional relation is shown in Figure 3. The numerical computations used to obtain the relation for $\hat{L}_{\text{sup max}}$ in Figure 3, as well as all other numerical computations reported here, were done by means of a strong stability-preserving (SSP) Runge-Kutta method of third order. The algorithm satisfies the TVD property necessary to preserve monotonicity of the numerical solution and avoid unphysical oscillations that often plague the results of ordinary Runge-Kutta methods (Gottlieb et al, 2001).

At any point \hat{x}_J where $0 \leq \hat{x}_J < \hat{L}_{\text{sup max}}$ the current may undergo a hydraulic jump to subcritical flow. Such jumps generally entrain little ambient water (e.g. Wilkinson & Wood, 1971; Stefan & Hayakawa, 1972; Baddour, 1987), so that the relations for conjugate Richardson number, flow velocity and flow thickness are given as

$$\mathbf{Ri}_{\text{cJ}} = \left[\frac{\sqrt{1+8/\mathbf{Ri}_J} - 1}{2} \right]^3 \mathbf{Ri}_J > 1 \quad (4.6a)$$

$$\frac{\hat{U}_{\text{cJ}}}{\hat{U}_J} = \left[\frac{\sqrt{1+8/\mathbf{Ri}_J} - 1}{2} \right]^{-1} < 1 \quad (4.6b)$$

$$\frac{\hat{h}_{\text{cJ}}}{\hat{h}_J} = \left[\frac{\sqrt{1+8/\mathbf{Ri}_J} - 1}{2} \right] > 1 \quad (4.6c)$$

where

$$\mathbf{Ri}_J = \mathbf{Ri} \Big|_{\hat{x}=\hat{x}_J} , \quad \hat{U}_J = \hat{U} \Big|_{\hat{x}=\hat{x}_J} , \quad \hat{h}_J = \hat{h} \Big|_{\hat{x}=\hat{x}_J} \quad (4.7a,b,c)$$

(Yih and Guha, 1955). These conjugate values define the boundary conditions for the conjugate subcritical flow downstream of the jump. The governing equations for this flow may be written as

$$\frac{d\tilde{U}}{d\tilde{x}} = \frac{-1 - \frac{e_w}{c_f} \left(1 + \frac{1}{2} \frac{\mathbf{Ri}_{cj}}{\tilde{U}^3}\right)}{1 - \frac{\mathbf{Ri}_{cj}}{\tilde{U}^3}} \frac{\tilde{U}}{\tilde{h}} \quad (4.8a)$$

$$\frac{d\tilde{h}}{d\tilde{x}} = \frac{1 + \frac{e_w}{c_f} \left(2 - \frac{1}{2} \frac{\mathbf{Ri}_{cj}}{\tilde{U}^3}\right)}{1 - \frac{\mathbf{Ri}_{cj}}{\tilde{U}^3}} \quad (4.8b)$$

where

$$\tilde{U} = \frac{U}{U_{cj}} = \frac{\hat{U}}{\hat{U}_{cj}} , \quad \tilde{h} = \frac{h}{h_{cj}} = \frac{\hat{h}}{\hat{h}_{cj}} , \quad \mathbf{Ri} = \frac{\mathbf{Ri}_{cj}}{\tilde{U}^3} , \quad \tilde{x} = \hat{x} - \hat{x}_J \quad (4.9a,b,c,d)$$

and U_{cj} and h_{cj} denote the dimensioned conjugate flow velocity and thickness, respectively. The boundary conditions on (4.8a) and (4.8b) are

$$\tilde{U} \Big|_{\tilde{x}=0} = 1 , \quad \tilde{h} \Big|_{\tilde{x}=0} = 1 \quad (4.10a,b)$$

Again the numerator of the right-hand side of (4.8a) is negative, but the denominator of the same must be negative as well, at least near $\tilde{x} = 0$. As a result \tilde{U} must increase monotonically in \tilde{x} until \mathbf{Ri} attains the value unity, at which the denominator of (4.8a) and (4.8b) become singular and the condition of a free overfall is reached. For any given values of $\mathbf{Ri}_{cj} > 1$ and c_f the distance \tilde{L}_{free} at which the free overfall is obtained can be computed, so that

$$\tilde{L}_{free} = \tilde{L}_{free}(\mathbf{Ri}_{cj}, c_f) \quad (4.11)$$

No solution to the subcritical problem is possible over domains \tilde{L} with lengths in excess of \tilde{L}_{free} .

Now for any value \hat{x}_J satisfying the condition $0 < \hat{x}_J < \hat{L}_{supmax}$ a complete solution which starts with the supercritical Richardson number $\mathbf{Ri}_o < 1$ at $\hat{x} = 0$, undergoes a hydraulic jump at \hat{x}_J and satisfies the free-overfall condition (3.8) at $\hat{x} = \hat{L}$

is obtained by a) solving (4.1a) and (4.1b) subject to (3.7a) and (3.7b) from $\hat{x} = 0$ to $\hat{x} = \hat{x}_J$, b) computing \mathbf{Ri}_{cJ} from (4.6), c) solving (4.8a) and (4.8b) subject to (4.10a) and (4.10b) from $\tilde{x} = 0$ to $\tilde{x} = \tilde{L}_{\text{free}}$ and d) computing \hat{L} as

$$\hat{L} = \hat{x}_J + \tilde{L}(\mathbf{Ri}_{cJ}, c_f) \quad (4.12)$$

For any given pair of values of $\mathbf{Ri}_o < 1$ and c_f and any specified value of \hat{x}_J , however, \mathbf{Ri}_{cJ} can be computed as a function of \hat{x}_J , \mathbf{Ri}_o and c_f . It follows, then, that (4.12) reduces to the form

$$\hat{L} = \hat{L}(\mathbf{Ri}_o, c_f, \hat{x}_J) \quad , \quad 0 \leq \hat{x}_J \leq \hat{L}_{\text{supmax}} \quad (4.13a,b)$$

Inverting the relation of (4.13),

$$\hat{x}_J = \hat{x}_J(\mathbf{Ri}_o, c_f, \hat{L}) \quad , \quad 0 \leq \hat{x}_J \leq \hat{L}_{\text{supmax}} \quad (4.14a,b)$$

The limits in (4.13) and (4.14) have specific physical meanings. When $\hat{x}_J = 0$ the hydraulic jump occurs precisely at the slope break of Figure 3, so that the conjugate Richardson number \mathbf{Ri}_{cJ} becomes equal to the conjugate Richardson number \mathbf{Ri}_{oJ} associated with the upstream Richardson number \mathbf{Ri}_o . In this case

$$\hat{L} = \tilde{L}_{\text{free}}(\mathbf{Ri}_{oJ}, c_f) \quad (4.15a)$$

$$\mathbf{Ri}_{oJ} = \left[\frac{\sqrt{1 + 8/\mathbf{Ri}_o} - 1}{2} \right]^3 \mathbf{Ri}_o > 1 \quad (4.15b)$$

For the case $\hat{L} > \tilde{L}_{\text{free}}(\mathbf{Ri}_{oJ}, c_f)$ it is found that $\hat{x}_J < 0$; the reach \hat{L} downstream of the slope break in Figure 3 is too long to support a hydraulic jump on it. Instead, the flow backs up and the jump occurs on the sloping region of Figure 2 upstream of the slope break. For the case $\hat{L} < \hat{L}_{\text{supmax}}(\mathbf{Ri}_o, c_f)$, on the other hand, the reach is too short for a hydraulic jump, and supercritical flow shoots off the free overfall without feeling it. These cases are illustrated in Figure 2.

Since for the case $\hat{x}_J = 0$ the value \mathbf{Ri}_{oJ} can be computed directly from \mathbf{Ri}_o from (4.15b), it follows that the maximum bound on \hat{L} , i.e. $\hat{L}_{\text{free}}(\mathbf{Ri}_{oJ}, c_f)$ can be computed from a knowledge of \mathbf{Ri}_o and c_f . With this in mind, a regime diagram for the occurrence of a hydraulic jump of a conservative underflow within the domain $0 \leq \hat{x} \leq \hat{L}$ is given in Figure 3.

A sample calculation is given in Figure 4. In the example the values of \mathbf{Ri}_o , and c_f are 0.2 and 0.005, respectively. For this case the value of $\hat{L}_{\text{sup max}}$ is found to be 0.1872. The jump is located so as to satisfy the condition $\hat{x}_j / \hat{L}_{\text{sup max}} = 0.6$. The values \mathbf{Ri}_j and \mathbf{Ri}_{c_j} are found to be 0.469 and 2.012, respectively. The value of \tilde{L}_{free} is computed as 0.0732, so that $\hat{L} = 0.6 \times 0.1872 + 0.0732 = 0.1855$. The computed profiles of \mathbf{Ri} , \hat{U} and \hat{h} are given in Figure 4.

For any given values of \mathbf{Ri}_o , c_f and \hat{L} it is necessary a) to determine whether it is possible for a hydraulic jump to occur on the domain $0 \leq \hat{x} \leq \hat{L}$, and if so b) to iterate for the value of \hat{x}_j within the bounds $0 \leq \hat{x}_j \leq \hat{L}_{\text{sup max}}$. The same iteration process that determines \hat{x}_j also determines the solutions to (4.1a) and (4.1b) on the supercritical reach and (4.8a) and (4.8b) on the subcritical reach.

5. The case of a purely depositional turbidity current with finite fall velocity

A turbidity current differs from a conservative bottom underflow in that the agent of the density difference, i.e. sediment, can exchange with the bed through erosion and deposition. Here the analysis of the previous section is extended to the case of a purely depositional turbidity current.

Supercritical flows are considered first. The equations to be solved are (3.4a) – (3.4c) subject to (3.7a) – (3.7c), and the further constraint $0 < \mathbf{Ri}_o < 1$. It was shown in the previous section that the case $v_s = 0$, or thus $\varphi = 0$ according to (3.6) has solutions such that $\mathbf{Ri} = 1$, and (3.4a) and (3.4b) become singular at $\hat{x} = \hat{L}_{\text{sup max}}(\mathbf{Ri}_o, c_f)$. It might be expected that $\hat{L}_{\text{sup max}}$ should change with increasing φ , and indeed it does. Of considerably more interest, however, is the fact that solutions attaining $\mathbf{Ri} = 1$ cease to exist when φ exceed a critical value $\varphi_{\text{supcrit}}(\mathbf{Ri}_o, c_f)$. Recalling the definition of φ from (3.6), the implication is that a sufficiently high fall velocity v_s (and thus deposition rate) renders a supercritical flow incapable of attaining the condition $\mathbf{Ri} = 1$.

To see this, the case $\mathbf{Ri}_o = 0.2$ and $c_f = 0.005$ is considered as an example. Plots of \mathbf{Ri} versus \hat{x} are given in Figure 5 for the cases $\varphi = 0, 0.5, 1, 1.389, 2, 4$ and 10 . Within the range $0 < \varphi < 1.389$ it is found that solutions attaining a singularity at $\mathbf{Ri} = 1$ do exist; the associated value $\hat{L}_{\text{sup max}}$ is found to be an increasing function of φ . Within the range $1.389 < \varphi$, however, a Richardson number of unity is never attained, and no singularity appears. That is, \mathbf{Ri} first increases above \mathbf{Ri}_o , reaches a maximum value less than unity, and thence declines monotonically toward zero.

The same general behavior is found for any combination (\mathbf{Ri}_o, c_f) under the constraint $\mathbf{Ri}_o < 1$. That is, a critical value

$$\varphi = \varphi_{\text{supcrit}}(\mathbf{Ri}_o, c_f) \quad (5.1)$$

exists such that within the range $0 \leq \varphi < \varphi_{\text{supcrit}}$ solutions exist such that \mathbf{Ri} attains unity at a singular point, and within the range $\varphi > \varphi_{\text{supcrit}}$ \mathbf{Ri} never attains unity and no singularity appears. A plot of φ_{supcrit} versus \mathbf{Ri}_o and c_f is given in Figure 6.

A point of interest in regard to Figure 5 concerns the profile of \mathbf{Ri} versus \hat{x} for $\varphi = \varphi_{\text{supcrit}}$. For this value of φ and only this value, the profile passes smoothly through $\mathbf{Ri} = 1$ without a singularity. This behavior is found to generalize to all values of \mathbf{Ri}_o and c_f .

The corresponding subcritical problem is obtained by solving (3.4a) – (3.4c) subject to (3.7a) – (3.7c), and the further constraint $\mathbf{Ri}_o > 1$. For the case $\varphi = 0$ it was shown in the previous section that the solutions attain the value $\mathbf{Ri} = 1$, where they become singular, at $\hat{x} = \hat{L}_{\text{free}}(\mathbf{Ri}_o, c_f)$. (Make the transformations $\hat{x} \rightarrow \tilde{x}$, $\hat{L}_{\text{free}} = \tilde{L}_{\text{free}}$ and $\mathbf{Ri}_o \rightarrow \mathbf{Ri}_{\text{cj}}$ in comparing with the material in the previous section on subcritical flows.). Again, it is found that a) \hat{L}_{free} increases with increasing φ , and b) as φ increases beyond a threshold value φ_{subcrit} the solutions fail to reach a Richardson number of unity and do not become singular anywhere. Profiles illustrating this are shown for the case $(\mathbf{Ri}_o, c_f) = (6, 0.005)$ in Figure 7; solutions become singular at $\mathbf{Ri} = 1$ for $0 < \varphi \leq \varphi_{\text{subcrit}} = 0.668$, but for $\varphi > \varphi_{\text{subcrit}}$ the Richardson attains a minimum value above unity, and then increases monotonically without any singularity. A plot of φ_{subcrit} versus \mathbf{Ri}_o and c_f is given in Figure 8.

As opposed to the case of supercritical flow, the subcritical solution remains singular at $\mathbf{Ri} = 1$ for every value of φ for which it attains the value $\mathbf{Ri} = 1$, including φ_{subcrit} .

6. Conditions for the impossibility of a hydraulic jump

The question of interest here is whether or not a turbidity current that is supercritical as it enters the domain $[0, L]$ of Figure 2 can undergo a hydraulic jump on that domain. It is of value to review the entire formulation for the case $\varphi > 0$. In the event that a jump can occur at some point \hat{x}_j , the flow is supercritical in the range $0 \leq \hat{x} \leq \hat{x}_j$ and subcritical on the domain $\hat{x} > \hat{x}_j$ or $\tilde{x} > 0$. Within the supercritical range the governing equations are (3.4a) – (3.4c) subject to (3.7a) = (3.7c) and the constraint $\mathbf{Ri}_o < 1$. Within the subcritical range the governing equations become

$$\frac{d\tilde{U}}{d\tilde{x}} = \frac{-1 - \frac{e_w}{c_f} \left(1 + \frac{1}{2} \mathbf{Ri}_{\text{cj}} \frac{\tilde{q}}{\tilde{U}^3} \right) + \frac{1}{2} \mathbf{Ri}_{\text{cj}} \frac{\tilde{q}}{\tilde{U}^4} \tilde{\varphi}}{1 - \mathbf{Ri}_{\text{cj}} \frac{\tilde{q}}{\tilde{U}^3}} \frac{\tilde{U}}{\tilde{h}} \quad (6.1a)$$

$$\frac{d\tilde{h}}{d\tilde{x}} = \frac{1 + \frac{e_w}{c_f} \left(2 - \frac{1}{2} \mathbf{Ri}_{cJ} \frac{\tilde{q}}{\tilde{U}^3} \right) - \frac{1}{2} \mathbf{Ri}_{cJ} \frac{\tilde{q}}{\tilde{U}^4} \tilde{\varphi}}{1 - \mathbf{Ri}_{cJ} \frac{\tilde{q}}{\tilde{U}^3}} \quad (6.1b)$$

$$\frac{d\tilde{q}}{d\tilde{x}} = -\tilde{\varphi} \frac{\tilde{q}}{\tilde{U}\tilde{h}} \quad (6.1c)$$

where

$$\tilde{U} = \frac{U}{U_{cJ}} = \frac{\hat{U}}{\hat{U}_{cJ}}, \quad \tilde{h} = \frac{h}{h_{cJ}} = \frac{\hat{h}}{\hat{h}_{cJ}}, \quad \tilde{q} = \frac{q}{q_J} = \frac{\hat{q}}{\hat{q}_J} \quad (6.2a,b,c)$$

$$\mathbf{Ri} = \frac{\mathbf{Ri}_{cJ}}{\tilde{U}^3}, \quad \tilde{x} = \hat{x} - \hat{x}_J \quad (6.2d,e)$$

$$\tilde{\varphi} = r_o \frac{v_s}{c_f U_{cJ}} = \frac{\varphi}{\hat{U}_{cJ}} \quad (6.3)$$

$$\mathbf{Ri}_{cJ} = \left[\frac{\sqrt{1 + 8/\mathbf{Ri}_J} - 1}{2} \right]^3 \mathbf{Ri}_J > 1 \quad (6.4a)$$

$$\frac{\hat{U}_{cJ}}{\hat{U}_J} = \left[\frac{\sqrt{1 + 8/\mathbf{Ri}_J} - 1}{2} \right]^{-1} < 1 \quad (6.4b)$$

$$\frac{\hat{h}_{cJ}}{\hat{h}_J} = \left[\frac{\sqrt{1 + 8/\mathbf{Ri}_J} - 1}{2} \right] > 1 \quad (6.4c)$$

$$\hat{q}_{cJ} = \hat{q}_J \quad (6.4d)$$

The boundary conditions on (6.1a) – (6.1c) are

$$\tilde{U}|_{\tilde{x}=0} = 1, \quad \tilde{h}|_{\tilde{x}=0} = 1, \quad \tilde{q}|_{\tilde{x}=0} = 1 \quad (6.5a,b,c)$$

The problem can be posed as follows. Let the values of c_f , φ and $\mathbf{Ri}_o < 1$ be specified. For these values, can any value \hat{L} be found such that a) the flow undergoes a hydraulic jump within the domain $0 < \hat{x} < \hat{L}$ and b) the resulting subcritical flow satisfies the free overfall condition stated below:

$$\mathbf{Ri}|_{\hat{x}=\hat{L}} = 1 \quad (6.6)$$

at the downstream end of the domain?

The solution can be implemented by solving the supercritical problem of (3.4) – (3.7) starting from any value $\mathbf{Ri}_o < 1$ for \mathbf{Ri} , \hat{U} , \hat{h} and \hat{q} as functions of \hat{x} , and asking

whether a hydraulic jump is possible at any value \hat{x} . The same solution that yields \mathbf{Ri} , \hat{U} , \hat{h} and \hat{q} as functions of \hat{x} also yields the conjugate Richardson number \mathbf{Ri}_c in accordance with (6.4a) and associated value $\tilde{\varphi}$ for the subcritical regime in accordance with (6.3) and (6.4b) (in both cases the subscript ‘‘J’’ has been omitted for simplicity). The subcritical problem is then defined by setting $\tilde{\varphi} = \tilde{\varphi}_J$ in (6.1a) – (6.1c) (with \mathbf{Ri}_c equated to \mathbf{Ri}_c).

The subcritical problem has a solution satisfying (6.6) only if

$$\tilde{\varphi} \leq \varphi_{\text{subcrit}} \quad (6.7)$$

For any given value c_f , it is possible to plot φ_{subcrit} as a function of \mathbf{Ri}_c in accordance with Figure 8. For the same value of c_f and specified values of \mathbf{Ri}_o and φ , the solution of (3.4a) - (3.4c) yields values of $\tilde{\varphi}$ and \mathbf{Ri}_c for every admissible value of \hat{x} . A plot of $\tilde{\varphi}$ and φ_{subcrit} versus \mathbf{Ri}_c reveals whether or not a solution exists. If $\tilde{\varphi}$ plots everywhere above φ_{subcrit} , then no solution with a hydraulic jump is possible, no matter what the value of \hat{L} .

A sample implementation of this procedure is given in Figure 9 for the case $\mathbf{Ri}_o = 0.3$ and $c_f = 0.005$. In addition to a plot of φ_{subcrit} versus \mathbf{Ri}_c , plots of $\tilde{\varphi}$ versus \mathbf{Ri}_c are given for the cases $\varphi = 0.5, 1.0, 1.668 (= \varphi_{\text{supcrit}})$ and 3. In the case $\varphi = 0.5$ it is seen that $\tilde{\varphi}$ plots below φ_{subcrit} over the entire range of values of \mathbf{Ri}_c , indicating that a value \hat{L} can be found such that hydraulic jump to a subcritical flow eventually attaining the condition $\mathbf{Ri} = 1$ is realized for all admissible values of \hat{x} , i.e. $0 \leq \hat{x} \leq \hat{L}_{\text{supmax}}$.

In the case $\varphi = 1.0$ of Figure 9, however, $\tilde{\varphi}$ plots above φ_{subcrit} for values of \mathbf{Ri}_c above 1.78. Within this range no hydraulic jump to a subcritical flow eventually satisfying the criterion $\mathbf{Ri} = 1$ is possible. In Figure 10, \mathbf{Ri} , \mathbf{Ri}_c and $\tilde{\varphi}$ of the supercritical solution are plotted versus \hat{x} for the case $\varphi = 1$. In addition, the value of \mathbf{Ri}_c is used to compute φ_{subcrit} as a function of \hat{x} for the same case of $\varphi = 1$. It is seen that the condition (6.7) ensuring the existence a hydraulic jump to subcritical flow eventually attaining the condition $\mathbf{Ri} = 1$ is satisfied only for the range $0.093 \leq \hat{x}_J \leq \hat{L}_{\text{supmax}}$, where in the present case $\hat{L}_{\text{supmax}} = 0.174$.

It is seen in Figure 9 that the case $\varphi = 1.638 = \varphi_{\text{supcrit}}$ corresponds to the threshold condition for the existence of a hydraulic jump to any solution eventually reaching $\mathbf{Ri} = 1$ for any \hat{L} . At this condition the lowest value of $\tilde{\varphi}$ (at $\mathbf{Ri} = \mathbf{Ri}_c = 1$) of 2.90 is precisely equal to the highest possible value of φ_{subcrit} . It is again seen from Figure 9 that when $\varphi = 2 > \varphi_{\text{supcrit}}$, $\tilde{\varphi}$ exceeds φ_{subcrit} everywhere, so that no solution with a hydraulic jump to subcritical flow eventually attaining $\mathbf{Ri} = 1$ is possible.

The above result is an extremely simple one. The threshold value φ_{nosol} of φ above which no solution exists such that the flow a) undergoes a hydraulic jump to subcritical flow and b) eventually attains the free overfall condition farther downstream can be stated as

$$\varphi_{\text{nosol}} = \varphi_{\text{supcrit}} \quad (6.8)$$

The above result generalizes. In Figure 11 $\tilde{\varphi}$ is plotted against \mathbf{Ri}_c for the case $c_f = 0.005$ and the values of $\mathbf{Ri}_o = 0.05, 0.075, 0.1, 0.15, 0.2, 0.3, 0.4, 0.5, 0.6, 0.7, 0.8$ and 0.9 , where for each value of \mathbf{Ri}_o φ has been set equal to the corresponding value of φ_{supcrit} . Also shown in the same plot is φ_{subcrit} versus \mathbf{Ri}_c . In every case the line of $\tilde{\varphi}$ versus \mathbf{Ri}_c plots above the curve for φ_{subcrit} versus \mathbf{Ri}_c , with the exception of the point $\mathbf{Ri}_c = 1$, where $\tilde{\varphi}$ becomes equal to φ_{subcrit} . The same result was obtained for values of c_f in the range $[0.001, 0.05]$. Thus the diagram of Figure 6, i.e. $\varphi_{\text{supcrit}}(\mathbf{Ri}_o, c_f)$ also specifies the threshold condition above which no hydraulic jump to a subcritical flow eventually satisfying the condition $\mathbf{Ri} = 1$ is possible.

7. Mathematical interpretation of the result

Figure 11 shows a feature that is too good to be true without reflecting some fundamental feature of the governing equations. For any given values of c_f , φ and starting value $\mathbf{Ri}_o < 1$ it is possible to compute \hat{U} , \hat{h} , \hat{q} and \mathbf{Ri} , and thus the conjugate values \hat{U}_c and \mathbf{Ri}_c versus \hat{x} according to (3.4a) – (3.4c), (3.5a), (4.6a) and (4.6b). (Again the subscript “J” has been omitted here for simplicity.). The solution allows one to determine e.g. the functional relations $\hat{U}(\mathbf{Ri}; \mathbf{Ri}_o, c_f, \varphi)$ and $\hat{U}_c(\mathbf{Ri}_c; \mathbf{Ri}_o, c_f, \varphi)$. Figure 11 specifically shows plots of the parameter $\tilde{\varphi}$ associated with the critical value φ_{supcrit} of φ for each value of \mathbf{Ri}_o . That is, it shows plots of

$$\tilde{\varphi} = \frac{\varphi_{\text{supcrit}}(\mathbf{Ri}_o, c_f)}{\hat{U}_c[\mathbf{Ri}_c; \mathbf{Ri}_o, c_f, \varphi_{\text{supcrit}}(\mathbf{Ri}_o, c_f)]} \quad (7.1)$$

for the case $c_f = 0.005$ and eleven values of \mathbf{Ri}_o ranging from 0.05 to 0.9. In all cases the lines plot one atop the other. The values of $\tilde{\varphi}$ defining this line plot everywhere above the maximum value of φ_{subcrit} , i.e.

$$\varphi_{\text{subcrit},1} \equiv \varphi_{\text{subcrit}}(\mathbf{Ri}, c_f) \Big|_{\mathbf{Ri}=1} \quad (7.2)$$

except for the point $\mathbf{Ri}_c = 1$, where $\tilde{\varphi} = \varphi_{\text{subcrit},1}$.

Since \mathbf{Ri}_c is related to \mathbf{Ri} and \hat{U}_c to \hat{U} by (4.6a) and (4.6b), respectively, the same collapse should show up in a plot of $\varphi_{\text{supcrit}}(\mathbf{Ri}_o, c_f) / \hat{U}(\mathbf{Ri}; \mathbf{Ri}_o, c_f)$. This is demonstrated in Figure 12, where $\varphi_{\text{supcrit}}(\mathbf{Ri}_o, c_f) / \hat{U}(\mathbf{Ri}; \mathbf{Ri}_o, c_f)$ is plotted against \mathbf{Ri} for $\mathbf{Ri}_o = 0.1, 0.4$ and 0.8 , and for $c_f = 0.001, 0.005$ and 0.05 .

For a given c_f the coincidence of all the lines in Figures 11 and 12 for a given value of c_f is a reflection of a similarity property of the governing equations, (3.4a) – (3.4c). As noted in the previous section, all supercritical solutions for \hat{U} and \hat{h} satisfying the condition of Figure 11, i.e. $\varphi = \varphi_{\text{supcrit}}(\mathbf{Ri}_o, c_f)$ pass through $\mathbf{Ri} = 1$ without a singularity. According to L'Hôpital's rule, the only way this can be possible in (3.4a) and (3.4b) is if the following condition is satisfied;

$$\frac{\varphi_{\text{supcrit}}(\mathbf{Ri}_o, c_f)}{\hat{U}[\mathbf{Ri}; \mathbf{Ri}_o, c_f, \varphi_{\text{supcrit}}(\mathbf{Ri}_o, c_f)]} = 2 \left(1 + \frac{3 e_{w1}}{2 c_f} \right) \quad (7.3)$$

where \hat{U}_1 is an abbreviation defined as

$$\hat{U}_1 \equiv \hat{U}[\mathbf{Ri}; \mathbf{Ri}_o, c_f, \varphi_{\text{supcrit}}(\mathbf{Ri}_o, c_f)] \Big|_{\mathbf{Ri}=1} \quad (7.4)$$

and according to (2.7)

$$e_{w1} \equiv e_w \Big|_{\mathbf{Ri}=1} = 0.00150 \quad (7.5)$$

Of interest first is the limiting case $\mathbf{Ri}_o \rightarrow 1$, in which case the calculation becomes degenerate (the solution begins and ends at $\hat{x} = 0$). In this case $\hat{U}_1 = \hat{U}_{c,1} = 1$, where $\hat{U}_{c,1}$ denotes the conjugate value of \hat{U}_1 , so that

$$\varphi_{\text{supcrit},1} \equiv [\varphi_{\text{supcrit}}(\mathbf{Ri}_o, c_f)] \Big|_{\mathbf{Ri}_o=1} = 2 \left(1 + \frac{3 e_{w1}}{2 c_f} \right) \quad (7.6)$$

By symmetry it follows that

$$\varphi_{\text{subcrit},1} = \varphi_{\text{subcrit}}(\mathbf{Ri}, c_f) \Big|_{\mathbf{Ri}=1} = \varphi_{\text{supcrit},1} = 2 \left(1 + \frac{3 e_{w1}}{2 c_f} \right) \quad (7.7)$$

In point of fact the values of φ_{supcrit} for the case $\mathbf{Ri} = 1$ in Figure 6 and φ_{subcrit} for the case $\mathbf{Ri} = 1$ in Figure 8, which were obtained numerically, correspond to the predictions of (7.6) and (7.7).

Now a supercritical solution for \hat{U} as a function of \mathbf{Ri} that a) satisfies the upstream boundary condition (3.7a) at $\mathbf{Ri} = \mathbf{Ri}_o$ and b) the condition (7.3) such that the solution pass through $\mathbf{Ri} = 1$ with no singularity can be written as

$$\hat{U} = \frac{\varphi_{\text{supcrit}}(\mathbf{Ri}_o, c_f)}{\varphi_{\text{supcrit}}(\mathbf{Ri}, c_f)} \quad (7.8)$$

In order to demonstrate that (7.8) is a solution, however, it also must be shown to satisfy (3.4a) – (3.4c). Setting $\varphi = \varphi_{\text{supcrit}}(\mathbf{Ri}_o, c_f)$, substituting (7.8) into the right-hand sides of (3.4a) – (3.4c), and reducing with (3.5a), the latter equations become

$$\frac{d\hat{U}}{d\hat{x}} = \frac{-1 - \frac{e_w}{c_f} \left(1 + \frac{1}{2} \mathbf{Ri}\right) + \frac{1}{2} \mathbf{Ri} \varphi_{\text{supcrit}}(\mathbf{Ri}, c_f)}{1 - \mathbf{Ri}} \frac{\hat{U}}{\hat{h}} \quad (7.9a)$$

$$\frac{d\hat{h}}{d\hat{x}} = \frac{1 + \frac{e_w}{c_f} \left(2 - \frac{1}{2} \mathbf{Ri}\right) - \frac{1}{2} \mathbf{Ri} \varphi_{\text{supcrit}}(\mathbf{Ri}, c_f)}{1 - \mathbf{Ri}} \quad (7.9b)$$

$$\frac{d\hat{q}}{d\hat{x}} = -\varphi_{\text{supcrit}}(\mathbf{Ri}, c_f) \frac{\hat{q}}{\hat{h}} \quad (7.9c)$$

subject to the same boundary conditions as before, i.e. (3.7a) – (3.7c). An inspection of (7.9a) – (7.9c) and (3.7a) – (3.7c) explains the collapse of the curves of Figure 11 and 12 into a single line for a given value of c_f ; the solution to the problem has collapsed into a single function of \mathbf{Ri} that is independent of the upstream Richardson number \mathbf{Ri}_o .

Further substituting (7.8) into the left-hand side of (7.9a) and reducing with (3.5a), it is found that

$$\begin{aligned} \frac{d\hat{U}}{d\hat{x}} &= -\frac{\varphi_{\text{supcrit}}(\mathbf{Ri}_o, c_f)}{\varphi_{\text{supcrit}}^2(\mathbf{Ri}, c_f)} \frac{d\varphi_{\text{supcrit}}}{d\mathbf{Ri}} \frac{d\mathbf{Ri}}{d\hat{x}} \\ &= \frac{-1 - \frac{e_w}{c_f} \left(1 + \frac{1}{2} \mathbf{Ri}\right) + \frac{1}{2} \mathbf{Ri} \varphi_{\text{supcrit}}(\mathbf{Ri}, c_f)}{1 - \mathbf{Ri}} \frac{1}{\hat{h}} \frac{\varphi_{\text{supcrit}}(\mathbf{Ri}_o, c_f)}{\varphi_{\text{supcrit}}(\mathbf{Ri}, c_f)} \end{aligned} \quad (7.10)$$

It is readily worked out from (3.4a) – (3.4c) and (3.5a) that

$$\frac{d\mathbf{Ri}}{d\hat{x}} = \frac{1 + \frac{e_w}{c_f} \left(1 + \frac{1}{2} \mathbf{Ri}\right) - \frac{1}{3} \left(1 + \frac{1}{2} \mathbf{Ri}\right) \frac{\varphi}{\hat{U}}}{1 - \mathbf{Ri}} \quad (7.11)$$

Reducing (7.11) with (7.8) and substituting into (7.10), a differential equation governing φ_{supcrit} as a function of \mathbf{Ri} is obtained such that (7.8) is indeed a solution to the problem. It takes the form

$$\frac{d\varphi_{\text{supcrit}}}{d\mathbf{Ri}} = \frac{1 + \frac{e_w}{c_f} \left(1 + \frac{1}{2}\mathbf{Ri}\right) - \frac{1}{2}\mathbf{Ri}\varphi_{\text{supcrit}}}{1 + \frac{e_w}{c_f} \left(1 + \frac{1}{2}\mathbf{Ri}\right) - \frac{1}{3} \left(1 + \frac{1}{2}\mathbf{Ri}\right)\varphi_{\text{supcrit}}} \quad (7.12)$$

The above equation provides a direct way to solve for φ_{supcrit} as a function of $\mathbf{Ri} \leq 1$ for any specified value of c_f . The boundary condition on (7.12) is seen from (7.6) to be

$$\varphi_{\text{supcrit}} \Big|_{\mathbf{Ri}_0=1} = 2 \left(1 + \frac{3 e_{w1}}{2 c_f} \right) \quad (7.13)$$

As might be expected, (7.12) is singular at $\mathbf{Ri} = 1$, but it is easily found with the use of L'hôpital's rule that where

$$\varphi'_1 \equiv \frac{d\varphi_{\text{supcrit}}}{d\mathbf{Ri}} \Big|_{\mathbf{Ri}=1}, \quad \varphi_1 \equiv \varphi_{\text{supcrit},1}, \quad r = \frac{1}{1.0204} \quad (7.14a,b,c)$$

the following equation is satisfied;

$$\varphi'_1 = \frac{-\frac{2e_{w1}}{c_f} \left(\frac{3}{2}r - \frac{1}{2}\right) + \left\{ \left[\frac{2e_{w1}}{c_f} \left(\frac{3}{2}r - \frac{1}{2}\right) \right]^2 + \frac{8}{3}\varphi_1 \left[\frac{e_{w1}}{c_f} \left(\frac{3}{2}r - \frac{1}{2}\right) + \frac{1}{2}\varphi_1 \right] \right\}^{1/2}}{2} \quad (7.15)$$

A numerical solution of (7.12) subject to (7.13) and (7.15) was found to yield the curves of Figure 6 (after transforming $\mathbf{Ri} \rightarrow \mathbf{Ri}_0$) within a fractional error of 0.002.

The curves of $\tilde{\varphi} = \varphi_{\text{supcrit}}(\mathbf{Ri}_0, c_f) / \hat{U}_c(\mathbf{Ri}_c; \mathbf{Ri}_0, c_f)$ versus \mathbf{Ri}_c in Figure 11 all plot above $\varphi_{\text{supcrit},1} = \varphi_{\text{subcrit},1}$ for $\mathbf{Ri}_c > 1$. From (6.4b) and (7.8) it is seen that

$$\tilde{\varphi} = \frac{\varphi_{\text{supcrit}}(\mathbf{Ri}_0, c_f)}{\hat{U}_c(\mathbf{Ri}_c; \mathbf{Ri}_0, c_f)} = \varphi_{\text{supcrit}}(\mathbf{Ri}, c_f) \frac{\sqrt{1 + 8/\mathbf{Ri}} - 1}{2} \quad (7.16)$$

It is easily demonstrated from (7.16) and the values of Figure 6 that

$$\varphi_{\text{supcrit}}(\mathbf{Ri}, c_f) \frac{\sqrt{1 + 8/\mathbf{Ri}} - 1}{2} \geq \varphi_{\text{supcrit},1} \quad (7.17)$$

with the equality holding only for the case $\mathbf{Ri} = 1$.

The criterion according to which the threshold condition for the existence of a hydraulic jump to a subcritical flow that eventually reaches a Richardson number of unity, i.e. $\varphi \leq \varphi_{\text{supcrit}}(\mathbf{Ri}_o, c_f)$ is seen to be built into the structure of the governing equations.

8. Physical interpretation of the result

The existence of a critical value of $\varphi = r_o v_s / (c_f U_o)$ above which no solution to the “jump problem” is possible merits an explanation in terms of the governing physics. Equations (2.2a) – (2.2c) reduce with the aid of (2.6), (2.8) - (2.10), the assumption of vanishing bed slope and the neglect of erosion of bed sediment to the steady forms

$$\frac{dU^2 h}{dx} = -\frac{1}{2} Rg \frac{d}{dx} \left(\frac{qh}{U} \right) - c_f U^2 \quad (8.1a)$$

$$\frac{dUh}{dx} = e_w U \quad (8.1b)$$

$$\frac{dq}{dx} = -r_o v_s \frac{q}{Uh} \quad (8.1c)$$

The problem of a conservative flow is recovered by setting $v_s = 0$. The first term on the right-hand side of (8.1a) is the term associated with the net streamwise force of the pressure gradient. Reducing it with (8.1c) yields the result

$$-\frac{1}{2} Rg \frac{d}{dx} \left(\frac{qh}{U} \right) = \frac{1}{2} r_o Rg v_s \frac{q}{U^2} - \frac{1}{2} Rgq \frac{d}{dx} \left(\frac{h}{U} \right) \quad (8.2)$$

The first term on the right-hand side of (8.2) is the term that generates the possibility of no solution to the “jump problem.” It represents a net accelerative force on the flow due to sediment deposition. That is, as sediment deposits out of the flow in accordance with (8.1c) the streamwise pressure force per unit width $(1/2) \rho RgCh^2 = (1/2) \rho Rgqh/U$ declines in the streamwise direction, generating a net positive force on any control volume.

Substituting (8.2) back in (8.1a) yields the relation

$$\frac{dU^2 h}{dx} = \frac{1}{2} r_o Rg v_s \frac{q}{U^2} - \frac{1}{2} Rgq \frac{d}{dx} \left(\frac{h}{U} \right) - c_f U^2 \quad (8.3)$$

in which the net accelerative effect on the flow due to sediment deposition is clear. Evidently the term containing the fall velocity suppresses the ability of a supercritical flow to decelerate toward a Richardson number of unity, and likewise suppresses the ability of a subcritical flow to accelerate toward a Richardson number of unity.

To see how a net force generated by sediment deposition that never changes sign can suppress the ability of some flows to decelerate and others to accelerate, it is necessary to reduce (8.3) a bit more. A reduction of (8.3) with (8.1b), (8.1c) and (2.8) gives the following form;

$$(1 - \mathbf{Ri}) \frac{h}{c_f U} \frac{dU}{dx} = \frac{1}{2} \mathbf{Ri} \frac{r_o}{c_f} \frac{v_s}{U} - \frac{e_w}{c_f} \left(1 + \frac{1}{2} \mathbf{Ri} \right) - 1 \quad (8.4)$$

In (8.4) the accelerative pressure term associated with sediment deposition has not changed sign. The effect of the other pressure term, i.e. the last term on the right-hand side of (8.2), however, is to generate a term $(1 - \mathbf{Ri})$ multiplying the spatial derivative of flow velocity in (8.4). For a supercritical flow $(1 - \mathbf{Ri})$ is positive, so that the pressure term associated with deposition adds a positive term to dU/dx and hinders the streamwise decrease in velocity as the flow decelerates toward $\mathbf{Ri} = 1$. For a subcritical flow $(1 - \mathbf{Ri})$ is negative, so the same term hinders the streamwise increase in velocity as the flow accelerates toward $\mathbf{Ri} = 1$. When the offending term is sufficiently strong, i.e. when $\varphi > \varphi_{\text{supcrit}}$ (supercritical flow) or $\varphi > \varphi_{\text{subcrit}}$ (subcritical flow), the suppressive effect of sediment deposition is so strong that a critical Richardson number cannot be reached.

9. Application at laboratory and field scale

The experiments of Garcia (1989) offer a means to test the criterion (6.8) for the occurrence of a hydraulic jump at a slope break. As noted in Section 1, these experiments correspond precisely to the configuration of Figure 2. Experiments were conducted with four grades of sediment, each with a different characteristic grain size D : NOVA ($D = 4 \mu\text{m}$), DAPER ($D = 9 \mu\text{m}$), GLASSA ($D = 30 \mu\text{m}$) and GLASSB ($D = 65 \mu\text{m}$), as shown in the Table. The kinematic viscosity of the water ν was computed from the water temperature θ given in the Table; the fall velocity v_s for each grade was then computed from a relation of Dietrich (1982) using the values for D , R and ν in the Table.

Direct measurements for the flow layer thicknesses h_o and layer-averaged flow velocities U_o and volume sediment concentration C_o at the slope break of Figure 2 are not reported in Garcia (1989). Kostic & Parker (2004; submitted), were, however, able to compute them upon calibrating a numerical model to the available data from Garcia (1989). Good fits to the available data were found for the value $c_f = 0.01$ for all experiments, and $r_o = 1$ for NOVA and DAPER and $r_o = 2$ for GLASSA and GLASSB. The computed values of h_o , U_o and C_o at the slope break are given in the Table, along with the assumed values of r_o . Also included in the table are the computed values of φ and φ_{subcrit} .

Garcia (1989) observed hydraulic jumps in all reported experiments using NOVA and DAPER. The formulation predicts these jumps, in that $\varphi < \varphi_{\text{supcrit}}$ in every case. Garcia did not observe hydraulic jumps in all reported experiments using GLASSA and

GLASSB. The formulation again predicts the absence of jumps, in that $\phi > \phi_{\text{supcrit}}$ in every case.

A sample application is offered here at field scale. The numbers are loosely based on calculations for the Amazon Submarine Fan by Pirmez and Imran (2003), but have been modified to reflect relatively swift flows emanating from the Amazon Submarine Canyon. The values of $(U_o, h_o, C_o, r_o, c_f, R)$ are taken to be (10 m/s, 50 m, 0.0124, 2.5, 0.002, 1.65); the values of \mathbf{Ri}_o and ϕ_{supcrit} are found to be 0.10 and 1.631. As grain size is varied from 50 to 250 μm fall velocity v_s (calculated from the relation of Dietrich, 1982 at 20° C for reference) varies from 0.22 to 3.04 cm/s, yielding values of ϕ ranging from 0.27 to 3.81. Based on these calculations a hydraulic jump to Richardson-critical flow is possible only for sediment finer than about 141 μm , as illustrated in Figure 13.

It should be pointed out that the above result applies only to a turbidity current carrying pure sand. It is likely that under some conditions a turbidity current is mostly driven by fine mud which does not readily deposit, but also carries a measurable fraction of sand which can exchange with the bed. Such a current may be able to undergo a hydraulic jump at a slope break while leaving a deposit of mostly sand.

10. Discussion

The theory presented above is formulated in the context of a layer-averaged model. Felix (in press) has suggested that layer-averaged models are inadequate in several ways to predict the characteristics of turbidity currents. The present model provides an excellent means of predicting the results of the experiments of Garcia (1989), as long as the parameters r_o and c_f can be first calibrated to the data. Formulations that preserve the vertical structure of the flow, such as that of Felix (1999) and Imran et al. (2004), however, have the advantage of predicting all the structure needed to infer a value of r_o . Peakall (2004) has pointed out that in general r_o can be expected to be a function flow conditions, as outlined in Parker (1982). A model that preserves the vertical structures of the flow allows this variation to be predicted as well.

The research presented here could thus be improved by moving from a layer-averaged model to one that includes both the vertical and transverse as well as streamwise structure of the flow. Work by Imran et al. (1998), Felix (2001) and Imran et al. (2004), for example, suggest avenues by which these generalizations might be accomplished.

Turbidity currents can entrain bed sediment as well as deposit sediment onto the bed. That is, the sediment entrainment coefficient e_s in (2.2c) and (2.11a-c) need not be zero. Kostic and Parker (2004; submitted) have studied the effect of including sediment entrainment in a model of the response of a turbidity current to a slope break. In correspondence to the work reported here, they have also found that sufficiently large values of the ratio v_s/U_o cause a turbidity current to traverse a slope break of the type of Figure 2 without undergoing a hydraulic jump. The similarity collapse reported in the

present work can no longer be obtained, however, when sediment entrainment is included in any realistic way.

The present analysis pertains to a quasi-steady turbidity current flowing over a prescribed bed with a slope break. Over time, however, the turbidity current would gradually change the bed profile through the deposition of sediment onto (or entrainment of sediment from) the bed. This morphodynamic evolution would occur over a time scale that is much longer than that required to set up the quasi-steady flow described here. The morphodynamics of turbidity current-bed interaction is considered in Kostic and Parker (2004; submitted). They have found that under the right conditions the turbidity current can leave a signature in the vicinity of the slope break in the form of a backward-facing step in the bed profile.

11. Conclusion

A 1D supercritical dense bottom flow flowing from a region with a positive bed slope onto a domain of vanishing slope ending in a free overfall (Figure 2) might be expected to undergo a hydraulic jump before reaching the free overfall. In the case of conservative flows driven by e.g. thermohaline effects, there is only one possible exception to this behavior; if the length L of the horizontal reach is too short, conditions for a jump may not be reached on the domain. (If the length L is too long the jump will occur on the sloping bed upstream of the transition, and the flow will no longer be supercritical at the transition).

Turbidity currents are non-conservative dense bottom flows, in that the agent of the density difference can change due to sediment entrainment from or deposition onto the bed. While Garcia (1989, 1993) was able to experimentally produce hydraulic jumps on the domain of Figure 2 with fine-grained (4 μm and 9 μm) turbidity currents, no hydraulic jump was evident for sufficiently coarse (30 μm and 65 μm) material, even though conditions were otherwise similar. The experiments suggest that under certain conditions the physics of the problem may render a hydraulic jump impossible for any length of domain, so that the “jump problem” described in the Introduction may have no solution.

In the case of purely depositional turbidity currents, the analysis yields a critical value of the dimensionless parameter $\phi = r_o v_s / (c_f U_o)$, where v_s denotes sediment fall velocity, c_f denotes bed friction coefficient, U_o denotes flow velocity at the slope break and r_o denotes the ratio of near-bed to layer-averaged suspended sediment concentration, above which the “jump problem” has no solution. This critical value $\phi_{\text{supercrit}}$ is an order-one parameter that is a function of the bulk Richardson number \mathbf{Ri}_o at the slope break and the friction coefficient c_f .

An application of the analysis to the results of Garcia (1989, 1993) essentially confirms the results found there. In the case of the 4 μm (NOVA) and 9 μm (DAPER) sediments, the inferred values of ϕ fall well below the critical values above which the “jump problem” has no solution. This corresponds with the fact that jumps were

observed for these experiments. In the case of 30 μm material (GLASSA), the inferred values of ϕ are about twice the critical values, in agreement with the fact that no jump was observed. In the case of the 65 μm material (GLASSB) the inferred values of ϕ are well above the critical values, again confirming the observation that no jumps were observed. A sample calculation illustrates how the methodology of the paper can be applied at field scale.

This material is based on work supported by a) ExxonMobil Upstream Research Corporation and b) the STC Program of the National Science Foundation under Agreement Number EAR-0120914. B. E. Prather and C. Pirmez, and their parent company Shell International Exploration and Production are sincerely thanked for introducing the authors to and allowing the reproduction of Figure 1.

REFERENCES

- ARMI, L. & FARMER, D. 1988 The flow of Mediterranean water through the Strait of Gibraltar. *Physical Oceanography* **21**(1), 1-105.
- BADDOUR, R. E. 1987 Hydraulics of shallow and stratified mixing channel. *J. Hydraul. Engrg.* **113**(5), 630-645.
- BAINES, P. G. 1999 Downslope flows into a stratified environment – structure and detrainment. In *Mixing and Dispersion in Stably Stratified Flows*, P.A. Davies (ed.), Oxford University Press, 1–20.
- BONNECAZE, R. T. & LISTER, J. R. 1999 Particle-driver gravity currents down planar slopes. *J. Fluid Mech.*, **390**, 75-91.
- CHOI, S. U. & GARCIA, M. 1995 Modeling of one-dimensional turbidity currents with a dissipative – Galerkin finite element method. *J. Hydraul. Res.* **33**, 623-647.
- DIETRICH, E. W. 1982 Settling velocity of natural particles. *Water Res. Res.* **18**(6), 1626-1982.
- ELLISON, T. H., & TURNER, J. S. 1959 Turbulent entrainment in stratified flows. *J. Fluid Mech.* **6**, 423-448.
- FELIX, M. 2001 A two-dimensional numerical model for a turbidity current. In *Particulate gravity currents*, Special Publication of the International Association of Sedimentologists **31**, McCaffrey, W. D., Kneller, B. C. & Peakall, J. (eds.), 71-81.
- FELIX, M. in press The significance of single value variables in turbidity currents. *J. Hydraul. Res.*
- FUKUSHIMA, Y, PARKER, G. & PANTIN, H. M. 1985 Prediction of ignitive turbidity currents in Scripps Submarine Canyon. *Marine Geology* **67**, 55-81.
- GARCIA, M. 1989 *Depositing and eroding sediment-drive flows: Turbidity currents*. Ph.D. Thesis, Department of Civil Engineering, University of Minnesota, Minneapolis.
- GARCIA, M. & PARKER, G. 1989 Experiments on hydraulic jumps in turbidity currents near a canyon-fan transition. *Science*, **245**, 393-396.
- GARCIA, M., 1993, Hydraulic jumps in sediment-driven bottom currents. *J. Hydraul. Engrg.* **119**(10), 1-24.

- GLADSTONE, C. & WOODS, A. 2000 On the application of box models to particle-driven gravity currents. *J. Fluid Mech.* **416**, 187-195.
- GOTTLIEB, S., SHU, C.W. & TADMOR, E. 2001 Strong stability-preserving high-order time discretization methods, *SIAM Journal of Numerical Analysis*, **43**, 89-112.
- HALLWORTH, M. A., HOGG, A. J. & HUPPERT, H. E. 1998 Effects of external flow on compositional and particle gravity currents. *J. Fluid Mech.* **359**, 109-142.
- IMRAN, J., PARKER, G. & KATOPODES, N. 1998 A numerical model of channel inception on submarine fans. *J. Geophys. Res. Oceans* **103**(C1), 1219-1238.
- IMRAN, J., KASSEM, A. & KHAN, S. M. 2004 Three-dimensional modeling of density current, I. flow in straight confined and unconfined channels. *J. Hydraul. Res.*, **42**(6).
- KOSTIC, S. & PARKER, G. 2003a Progradational sand-mud deltas in lakes and reservoirs: Part 1. Theory and numerical modeling. *J. Hydraul. Res.*, **41**(2), 127-140.
- KOSTIC, S. & PARKER, G. 2003b Progradational sand-mud deltas in lakes and reservoirs: Part 2. Experiment and numerical simulation. *J. Hydraul. Res.*, **41**(2), 141-152.
- KOSTIC, S. & PARKER, G. 2004 Can an internal hydraulic jump be inferred from the depositional record of a turbidity current? *Proceedings, RiverFlow 2004 International Conference on Fluvial Hydraulics, Napoli, Italy, June 23-25*, 9 p.
- KOSTIC, S. & PARKER, G. submitted The response of turbidity currents to a canyon-fan transition: internal hydraulic jumps and depositional signatures. *J. Hydraul. Res.*
- LANE-SERFF, G. F., SMEED, D. A. & POSTLETHWAITE, C. R. 2000 Multi-layer hydraulic exchange flows. *J. Fluid Mech.* **41**, 269-296.
- MAXWORTHY, T. 1999 The dynamics of sedimenting surface gravity currents. *J. Fluid Mech.* **392**, 27-44.
- MUTTI, E. 1977 Distinctive thin-bedded turbidite facies and related depositional environments in the Eocene Hecho Group (South-central Pyrenees, Spain). *Sedimentology* **24**, 107-131.
- PARKER, G. 1982 Conditions for the ignition of catastrophically erosive turbidity currents. *Marine Geology* **46**, 307-327.
- PARKER, G., FUKUSHIMA, Y. & PANTIN, H.M. 1986 Self-accelerating turbidity currents, *J. Fluid Mech.* **171**, 145-181.
- PARKER, G., GARCIA, M. H., FUKUSHIMA, Y. & YU, W. 1987 Experiments on turbidity currents over an erodible bed. *Journal of Hydraulic Research*, **25**(1) 123-147,
- PEAKALL, J. 2004 Personal communication.
- PIRMEZ, C. & IMRAN, J. 2003 Reconstruction of turbidity currents in a meandering submarine channel. *Marine and Petroleum Geology* **20**(6-8), 823-849.
- RUSSELL, H. A. J. & ARNOTT, R. W. C. 2003 Hydraulic-jump and hyperconcentrated-flow deposits of a glacialigenic subaqueous fan: oak ridges moraine, southern Ontario, Canada. *J. Sedimentary Res.*, **73**(6), 887-905.
- STEFAN, H. & HAYAKAWA, N. 1972 Mixing induced by an internal hydraulic jump. *Water Res. Bull.*, **8**(3), 531-545.
- WILKINSON, D. L. & WOOD, I. R. 1971 A rapidly varied flow phenomenon in a two-layer flow. *J. Fluid Mech.*, **47**(2), 241-256.
- YIH, C. S. & GUHA, C. R. 1955 Hydraulic jumps in a fluid system of two layers, *Tellus* **7**(3), 358-366.

Table
 Test of the Criterion for a Hydraulic Jump Versus the Experimental Data of Garcia (1989)

EXP.	h_0 (m)	U_0 (m/s)	C_0 $\times 10^3$	R	Ri_0	D_{50} (μm)	θ ($^\circ\text{C}$)	v $\times 10^7$ (m^2/s)	v_s $\times 10^5$ (m/s)	r_0	ϕ	ϕ_{supert}	Predicted	Observed
NOVA1	0.078	0.064	0.664	1.65	0.203	4	25.5	8.93	1.15	1	0.018	1.282	jump	jump
NOVA2	0.065	0.071	0.985	1.65	0.208	4	25.0	9.04	1.14	1	0.016	1.295	jump	jump
NOVA4	0.066	0.099	2.159	1.65	0.236	4	25.0	9.04	1.14	1	0.011	1.358	jump	jump
DAPER1	0.078	0.061	0.671	1.65	0.225	9	26.0	8.83	7.31	1	0.119	1.333	jump	jump
DAPER2	0.079	0.060	0.632	1.65	0.221	9	26.0	8.83	7.31	1	0.121	1.324	jump	jump
DAPER4	0.063	0.085	0.132	1.65	0.187	9	26.5	8.73	7.41	1	0.088	1.244	jump	jump
DAPER6	0.060	0.090	1.627	1.65	0.196	9	25.5	8.93	7.21	1	0.080	1.267	jump	jump
DAPER7	0.060	0.101	3.344	1.65	0.318	9	23.0	9.44	6.77	1	0.067	1.526	jump	jump
GLASSA1	0.137	0.039	0.087	1.50	0.128	30	25.5	8.93	8.31	2	4.276	1.089	no jump	no jump
GLASSA2	0.114	0.049	0.186	1.50	0.145	30	26.0	8.83	8.40	2	3.458	1.137	no jump	no jump
GLASSA4	0.119	0.046	0.155	1.50	0.141	30	26.0	8.83	8.40	2	3.657	1.126	no jump	no jump
GLASSA5	0.110	0.051	0.218	1.50	0.149	30	26.0	8.83	8.40	2	3.289	1.148	no jump	no jump
GLASSA7	0.120	0.057	0.262	1.50	0.157	30	26.0	8.83	8.40	2	2.944	1.168	no jump	no jump
GLASSA9	0.098	0.076	0.637	1.50	0.176	30	26.5	8.73	8.50	2	2.244	1.216	no jump	no jump
GLASSB1	0.305	0.033	0.005	1.50	0.023	65	25.0	9.04	3.54	2	21.74	none	no jump	no jump
GLASSB2	0.254	0.040	0.013	1.50	0.034	65	23.5	9.34	3.44	2	17.32	0.067	no jump	no jump
GLASSB3	0.339	0.029	0.003	1.50	0.019	65	23.0	9.44	3.41	2	23.48	none	no jump	no jump

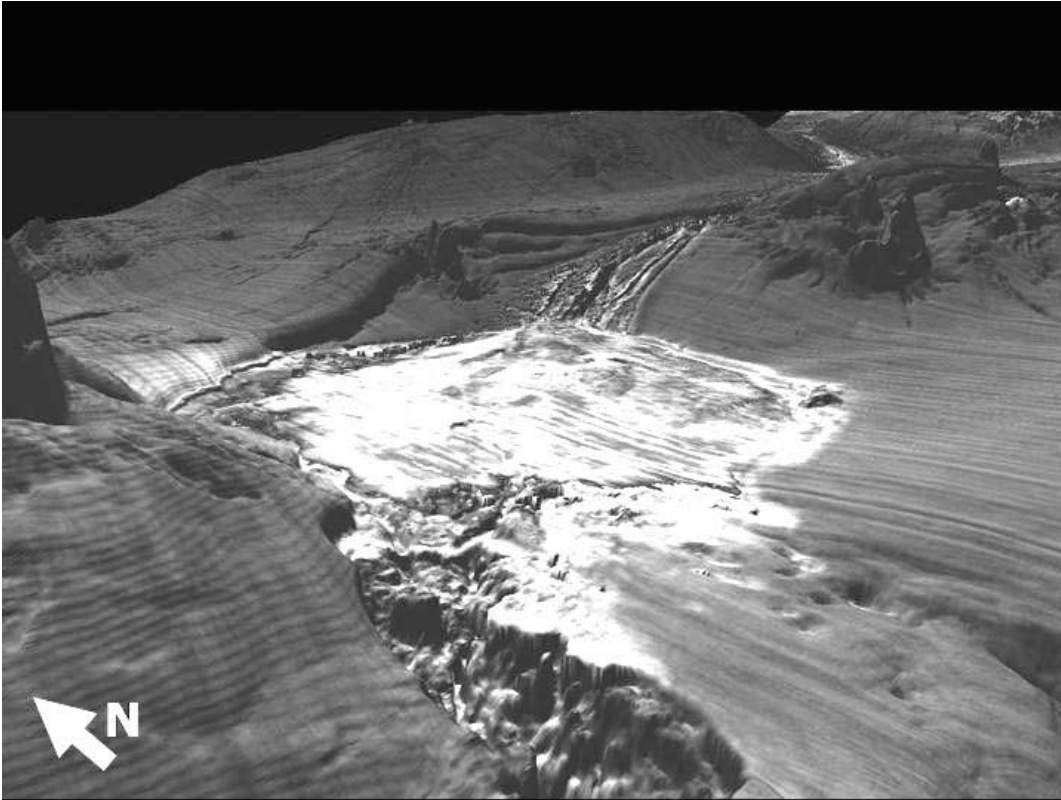


Figure 1 Seismic image looking upstream at a submarine canyon/fan/canyon complex on the continental slope off the Niger River, Africa. The zone between the upstream canyon and the fan is a zone of decreasing bed slope, creating conditions that could cause a turbidity current to undergo an internal hydraulic jump. Image courtesy B. Prather and C. Pirmez.

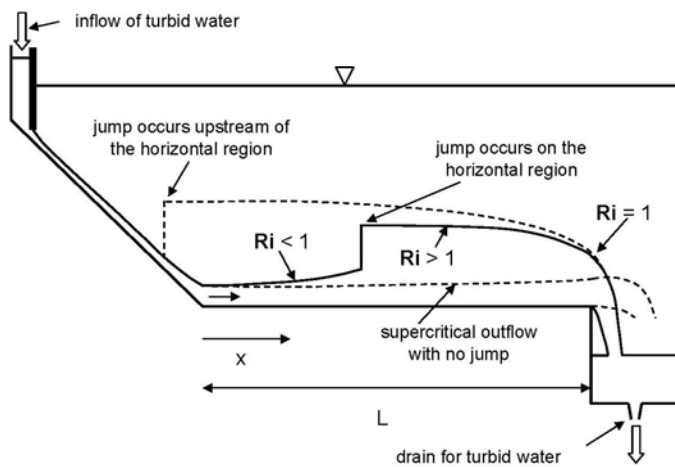


Figure 2 Experimental configuration of Garcia (1989).

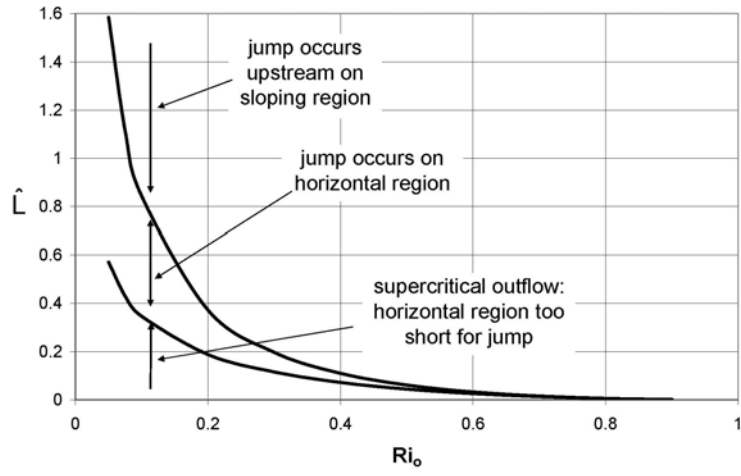


Figure 3 Regime diagram for a hydraulic jump of a conservative underflow.

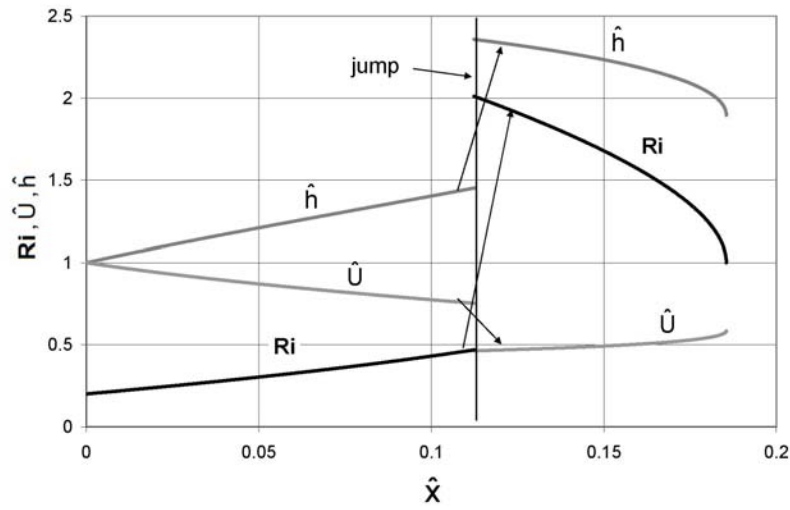


Figure 4 Results of a sample calculation for a conservative underflow which undergoes a hydraulic jump.

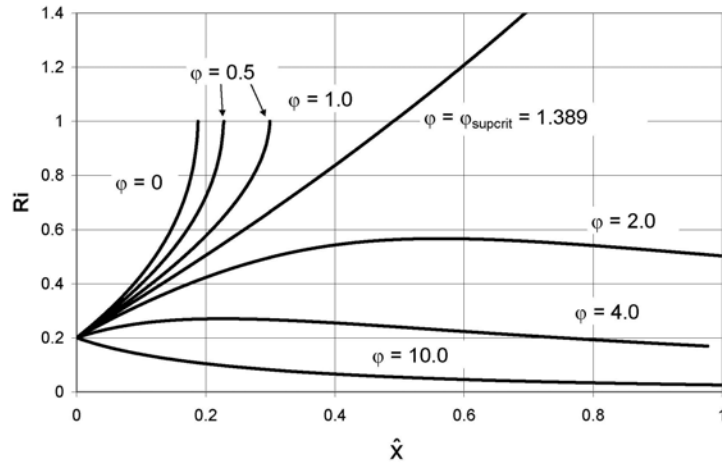


Figure 5 Calculations of Ri versus \hat{x} for supercritical depositional turbidity currents with various values of ϕ , all with an upstream value $Ri_o = 0.2$ and a value of c_f of 0.005. For $\phi > \phi_{supercrit}$ the turbidity current is unable to attain a value of Ri of 1 anywhere.

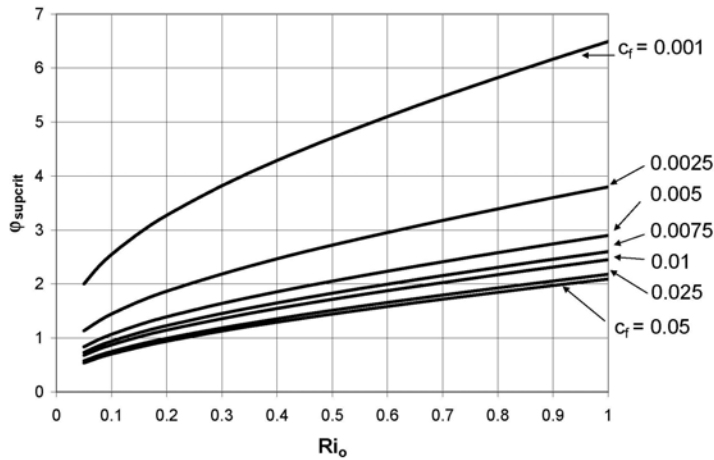


Figure 6 Plot of $\phi_{supercrit}$ versus Ri_o for various values of c_f .

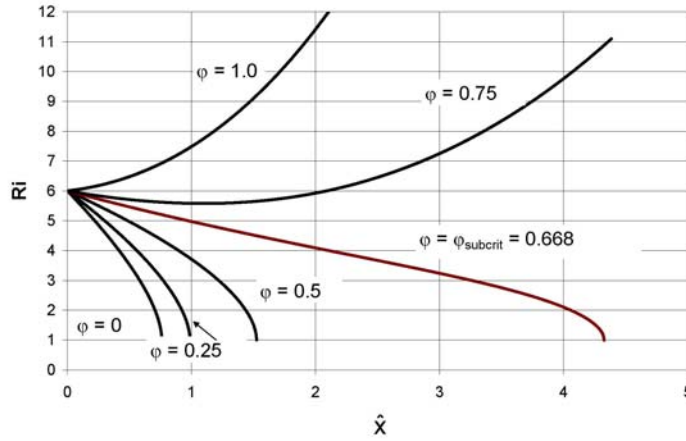


Figure 7 Calculations of \mathbf{Ri} versus \hat{x} for subcritical depositional turbidity currents with various values of ϕ , all with an upstream value of \mathbf{Ri} of 6.00 and a value of c_f of 0.005. For $\phi > \phi_{\text{subcrit}}$ the turbidity current is unable to attain a value of \mathbf{Ri} of 1 anywhere.

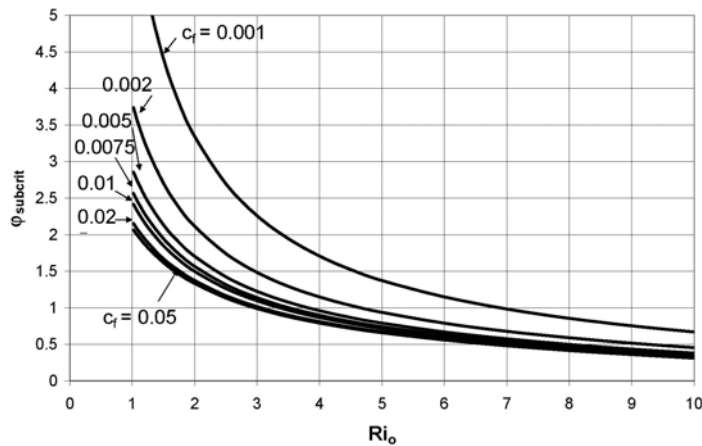


Figure 8 Plot of ϕ_{subcrit} versus \mathbf{Ri}_o for various values of c_f .

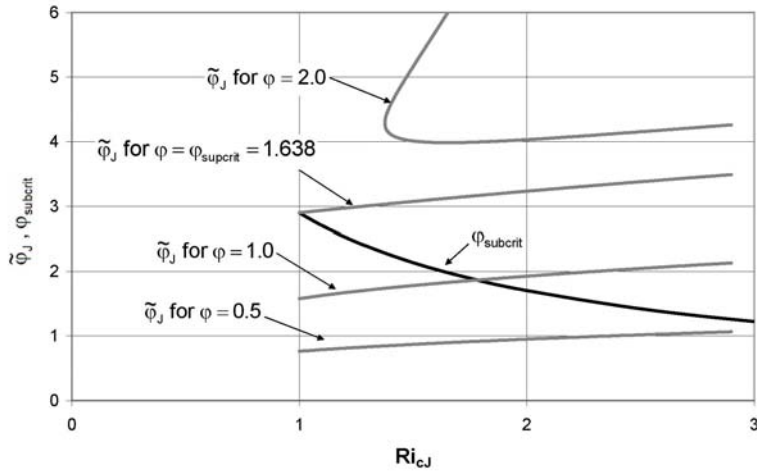


Figure 9 Plots of $\tilde{\varphi}_J$ versus \mathbf{Ri}_{cJ} for various values of φ and the values $\mathbf{Ri}_0 = 0.3$ and $c_f = 0.005$. Also plotted is $\tilde{\varphi}_J$ versus \mathbf{Ri}_{cJ} for the case $c_f = 0.005$. No hydraulic jump to subcritical flow is possible when $\tilde{\varphi}_J > \varphi_{subcrit}$ for all \mathbf{Ri}_{cJ} .

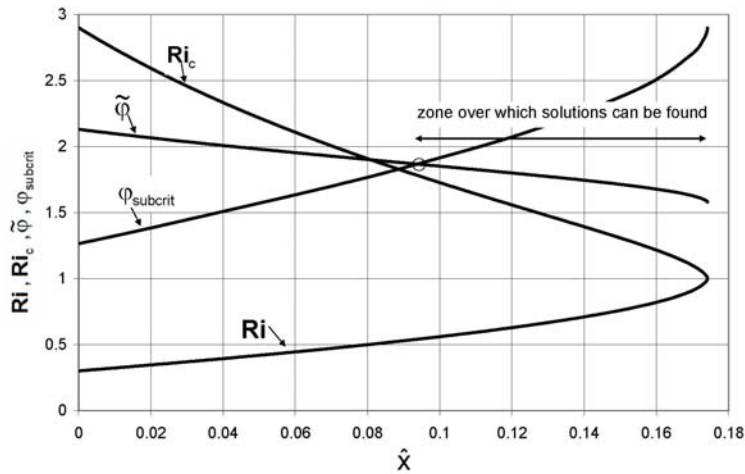


Figure 10 Plot of \mathbf{Ri} , $\tilde{\varphi}$, $\varphi_{subcrit}$ and \mathbf{Ri}_c versus \hat{x} for the case $\mathbf{Ri}_0 = 0.3$ and $c_f = 0.005$. Solutions to the jump problem can only be found only by locating the jump at a value $\hat{x} = \hat{x}_j$ for which $\tilde{\varphi} \leq \varphi_{subcrit}$.

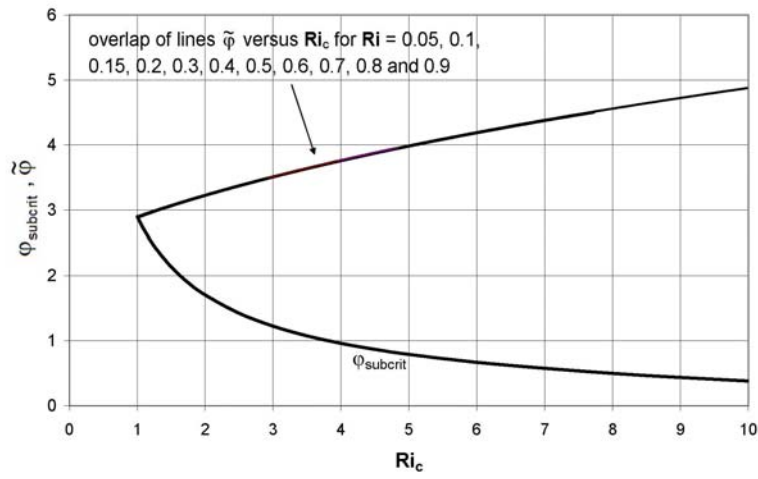


Figure 11 The figure shows plots of $\tilde{\varphi} = \varphi_{\text{supcrit}}(\mathbf{Ri}_o, c_f) / \hat{U}_c[\mathbf{Ri}_c; \mathbf{Ri}_o, c_f, \varphi_{\text{supcrit}}(\mathbf{Ri}_o, c_f)]$ for the case $c_f = 0.005$ and eleven values of \mathbf{Ri}_o ranging from 0.05 to 0.9. Also shown is the plot of φ_{subcrit} versus \mathbf{Ri}_c for the same value of c_f . The lines of $\tilde{\varphi}$ versus \mathbf{Ri}_c are seen to collapse on top of each other.

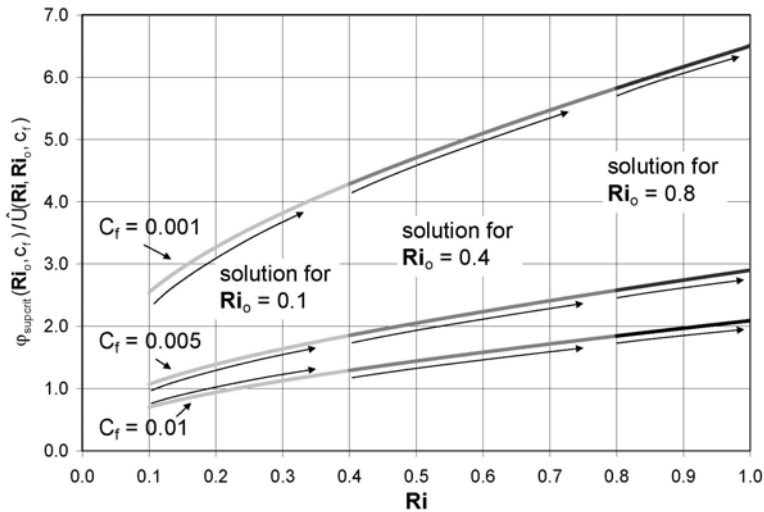


Figure 12 In this figure $\varphi_{\text{supcrit}}(\mathbf{Ri}_o, c_f) / \hat{U}(\mathbf{Ri}; \mathbf{Ri}_o, c_f)$ is plotted against \mathbf{Ri} for $\mathbf{Ri}_o = 0.1, 0.4$ and 0.8 for $c_f = 0.001, 0.005$ and 0.05 . All lines are seen to collapse on top of each other for a given value of c_f .

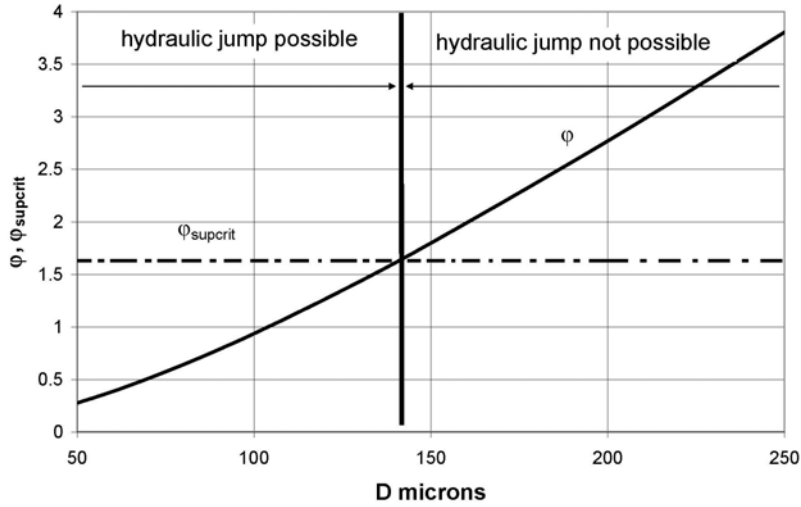


Figure 13 Plot of ϕ and ϕ_{supcrit} versus grain size D for a current with the values $(U_o, h_o, C_o, r_o, c_f, R) = (10 \text{ m/s}, 50 \text{ m}, 0.0124, 2.5, 0.002, 1.65)$ and a water temperature θ of 20° C . These values yield in turn the values $(\mathbf{Ri}_o, \phi_{\text{supcrit}}) = (0.10, 1.631)$. The plot shows that a hydraulic jump to Richardson-subcritical flow is possible only for a turbidity current driven by sediment finer than about $141 \mu\text{m}$.